Introduction

Fluid flow through different microchannels was observed to analyze microfluid, or “beads” behaviours in various patterns, such as straight, curved, and widening regions. A Leica DMI4000 Inverted Microscope was used to observe the fluid. Streaklines, or simply streaks, were analyzed to study the velocity behaviour of fluids in changing parameters, such as the distance to the sidewall, pressure, and geometry of the channels.

Experimental Procedures and Results

For the most part, the procedure from the Microfluidics Lab Manual [1] was followed. However, due to time constraints, the hemocytometer was not used. Instead, a pixel counting tool [2] and the default scale were used to determine the length of streaks. For example, if the length of a streak was 40% of the length of the $100\mu m$ scale, the streak’s length was $40\mu m$. Multiple uncertainties affect the determination of the streak length and flow velocity. These are discussed in detail in *Error Analysis.*

Flow through four channels were observed (Fig. 1). A straight portion of channel 1 was used to generate a velocity profile of the fluid. Channels 1 and 2 both contain a widening region, but one is abrupt and the other is gradual. The differences and similarities in fluid behaviour between these regions were observed. The amount of fluid in the syringe was also adjusted, and the any differences in fluid velocity were detected.

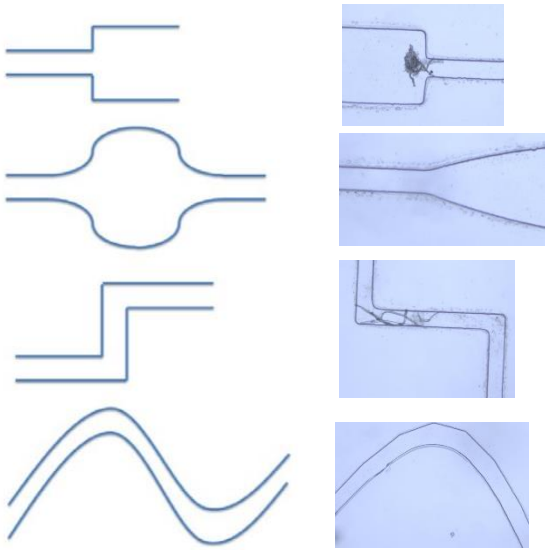

(Fig. 1) From top to bottom, channels 1, 2, 3, and 4. Beside are the actual profile of the channel as viewed under the Leica DMI4000.

Smoothness of Channel Sidewalls

The sidewalls were relatively smooth under 400X magnification. There were some minor imperfections, namely portions that were not perfectly straight and contained small bumps.

These imperfections impacted fluid flow by causing minor turbulences. However, these disturbances were not empirically observed.

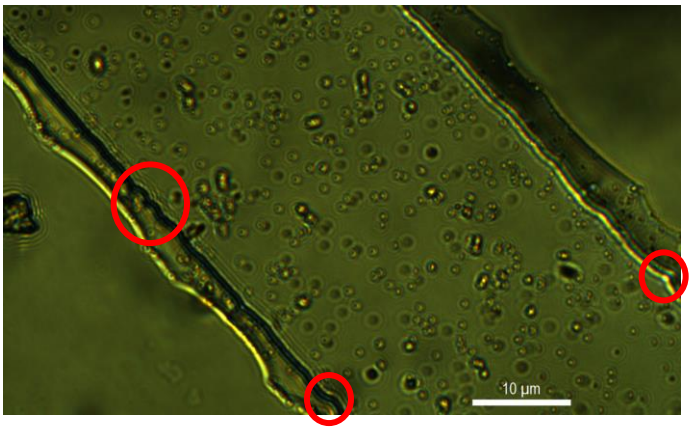

(Fig. 2) Some imperfections, highlighted in red, were noticeable at 400X magnification.

Straight Channels

For channel 1, the largest velocity is expected to be at the center of the channel before it widened. Velocity is greater near the centre than the edges since there are frictional forces between the channel walls and the fluid. In fact, the fluid velocity at the walls is zero. Larger velocity is also expected at regions with small cross-sectional area due to their inverse relationship: $A_1 v_1 = A_2 v_2$. This equation is obeyed throughout the length of any channel.

Laminar flow was observed as the flow was constant through time. The streaks, representing the path of the beads through time, were parallel to the channel walls and no eddies were formed.

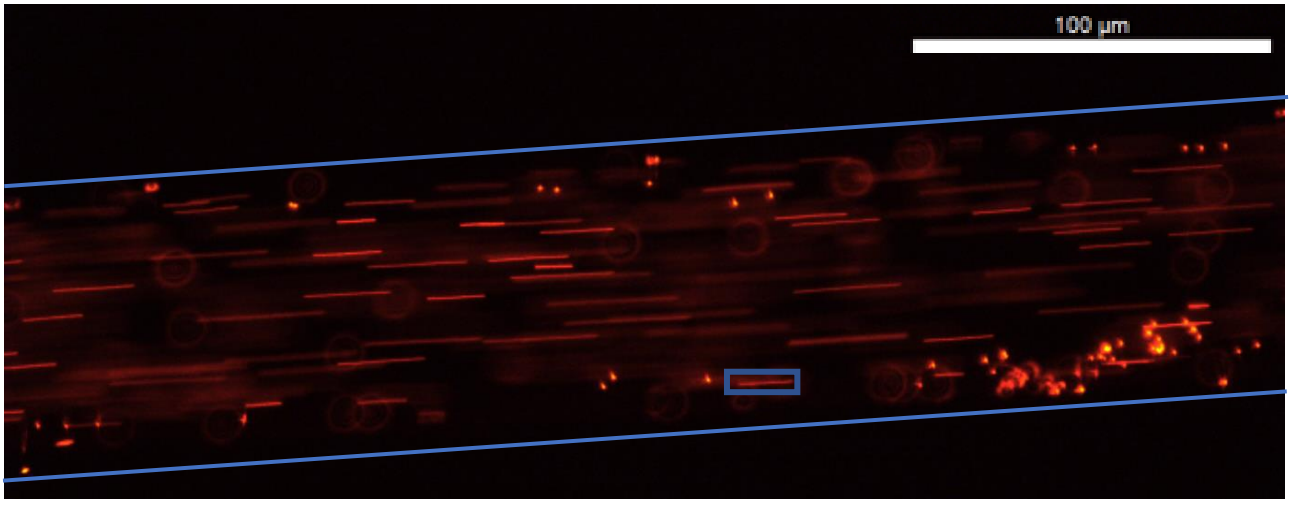

(Fig. 3) The streaks of a portion of the straight channel. The parallel blue lines indicate the channel sidewalls. Notice the streak lengths were not uniform and, in general, streaks near the middle of the channel were longer than those near the walls.

To find the velocity profile, the lengths of multiple streaks across the width of the channel were calculated. Streaks that were less blurry and whose beginning and end were clearly visible were

selected to minimize uncertainties. Velocity, v was determined by $v = l/t$, where l is the length of the streak and t is the exposure time, which was $50.6 \pm 0.1ms$ for this image. A pixel counter tool [2] was used to determine the length of each streak. As an example, consider the streak in Fig. 3 boxed in blue. It contained 93 ± 2 pixels. The 100µm scale contained 613 ± 12 pixels. The length of this streakline is therefore $93/613 * 100\mu m = 15.2 \pm 0.343\mu m$. Finally, the velocity is $v = 15.2\mu m/50.6ms = 0.300 \pm 0.00681mm/s$. The derivations in *Error Analysis* contain the explanation for the given errors. This procedure was followed to obtain distance and velocity data for 32 streaks in Fig 3. These were plotted to generate the velocity profile shown below (Fig. 4).

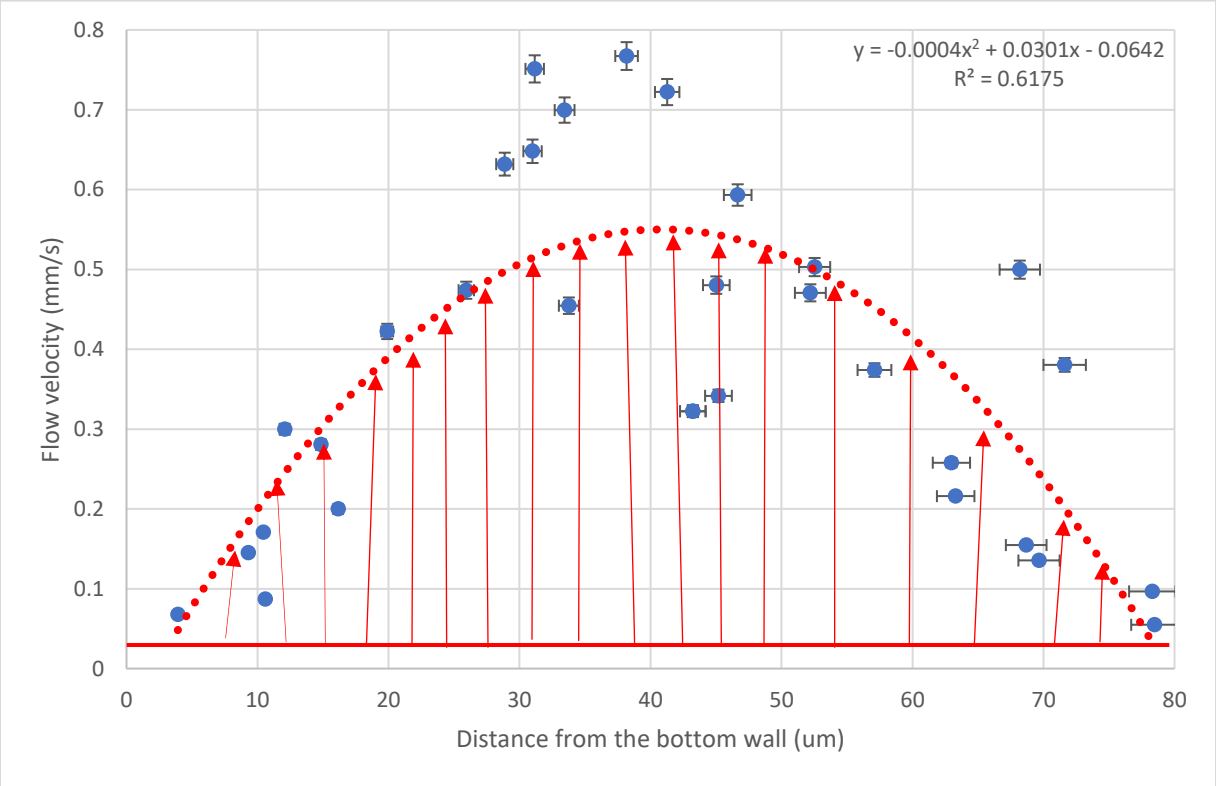

(Fig. 4) Velocity profile describing the flow in Fig. 3. Error bars were placed according to the error formulae derived in *Error Analysis*. Note that the velocity profile should be rotated left by 90 degrees to match Fig. 3's channel orientation.

The velocity is at a maximum at the centre of the channel, and very small near both ends. A parabolic curve of best fit was used – velocity increases proportional to the square of the distance from the wall. The relationship between velocity and distance from the wall was not strong, as indicated by the small R value. The variation was not within measurement uncertainties. This was likely due to the limitations in the camera. However, the general trend that velocity near the middle of the channel is greater is clear.

Bernoulli's principle governs fluid flow and it is given by $P_1 + \frac{1}{2}\rho v_1^2 + \rho g h_1 = P_2 + \frac{1}{2}\rho v_2^2 + \rho g h_2$, where P is the pressure, ρ is the fluid density, v is the velocity, g is the acceleration due to

gravity, and h is the reference height. For the context of this experiment, the inlet velocity is 0 and the initial pressure is due to the fluid's weight. Bernoulli's equation simplifies to $\frac{mg}{A} + \rho g h_1 = P_2 + \frac{1}{2}\rho v_2^2$. As the amount of fluid increases, m and h_1 both increase. By Bernoulli's equation, the flow velocity, v_2 also increases. This was indeed observed in practice: as we increased the amount of fluid in the syringe, a visible increase in the length of streaks were observed, signifying a velocity increase. We also took advantage of Bernoulli's equation to control the size of streaks. For example, if the streaks were too long, we lowered the gravity head to get shorter streaks.

Channels of Different Sizes

As channel widths increase, velocity will decrease. The formula that governs the relationship between channel size and flow velocity is $A_1 v_1 = A_2 v_2$, where A is the cross-sectional area and v is the velocity. Here, we assume that the channel height does not change, so the equation simplifies to $w_1 v_1 = w_2 v_2$, where w is the width of the channel. To verify this relationship, two streaks from Fig. 5a, boxed in blue, were sampled. They were approximate equidistant from the sidewall. For the narrower channel, $w_1 v_1 = 63 * 21 = 1323$, where both w and v were measured in pixels. After the channel widens, $w_2 v_2 = 129 * 11 = 1419$. These two values agree to 7%, which is good evidence that the area-velocity relationship is satisfied.

Abrupt transitions (Fig. 5b) resulted in a turbulence region. Gradual transitions (Fig. 5a) eliminated the turbulence region after widening. Turbulence is signified by the patch of bright spots after the widening of the second channel. Notice that no streaks can be discerned. This is because the flow is random and in all directions.

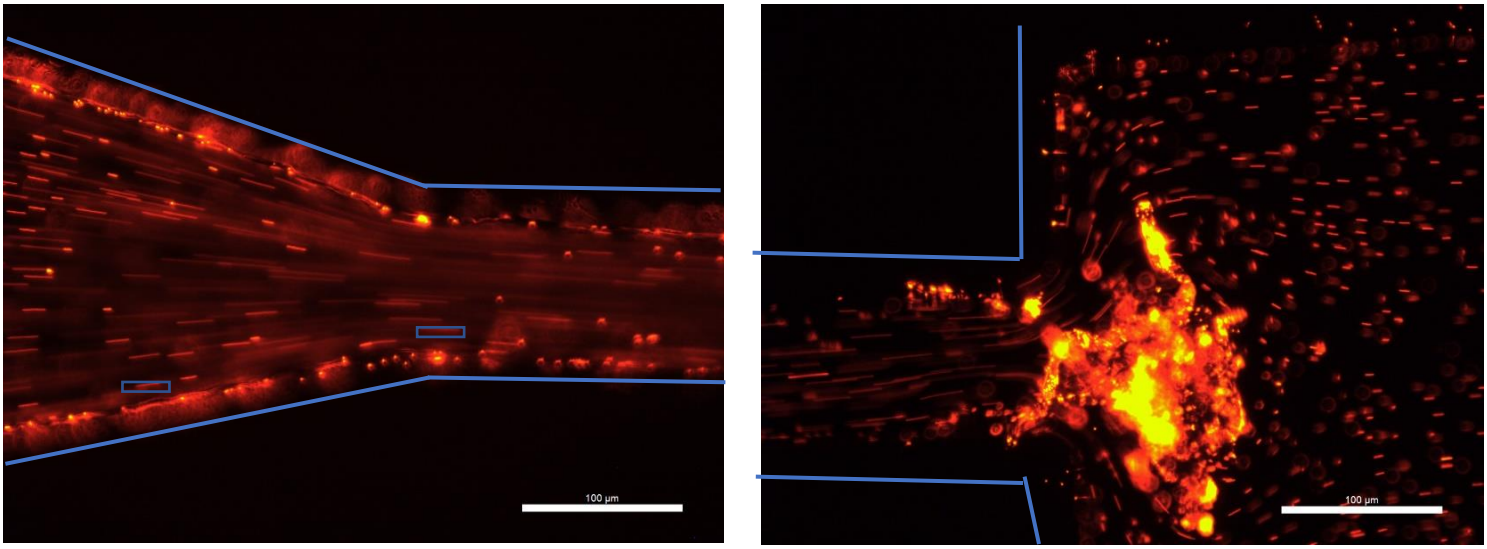

Fig. 5a (left) and Fig. 5b (right) The flow through a gradually widening and abruptly widening channel. Note the turbulence after the channel widening in 5b. To enhance visibility, channel sidewalls are highlighted in blue.

Bends in Channels

For channels 3 and 4, there was a noticeable velocity decrease during the bend. The velocity returned to the previous velocity after the bend. Velocity decrease in the gentle bend (Fig. 6b) was much less pronounced. Turbulent flow was observed at the elbow and after the sharp bend (Fig. 6a).

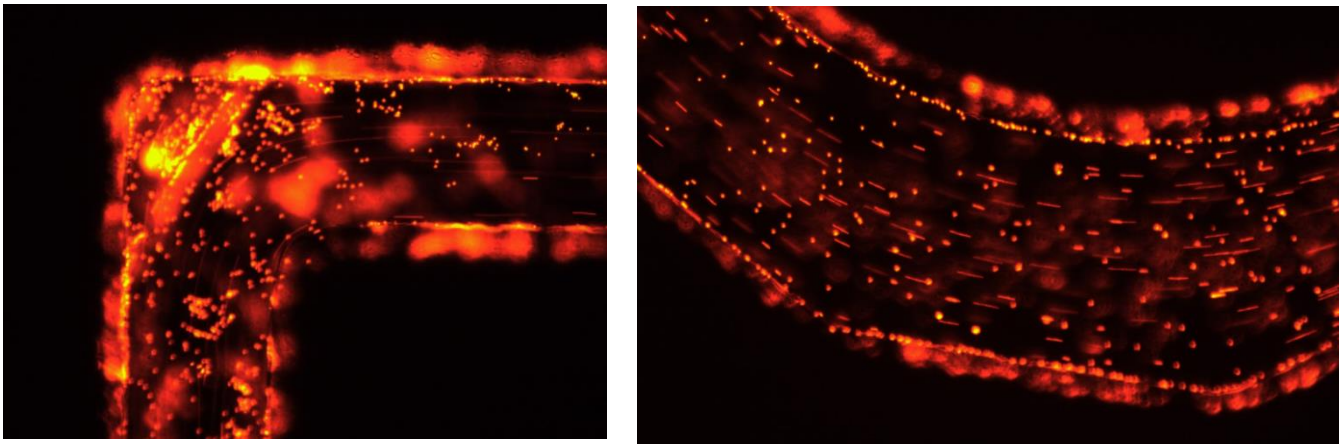

Fig. 6a (left) and 6b (right) The flow through a sharp bend was turbulent whereas the flow through the gentle bend was laminar.

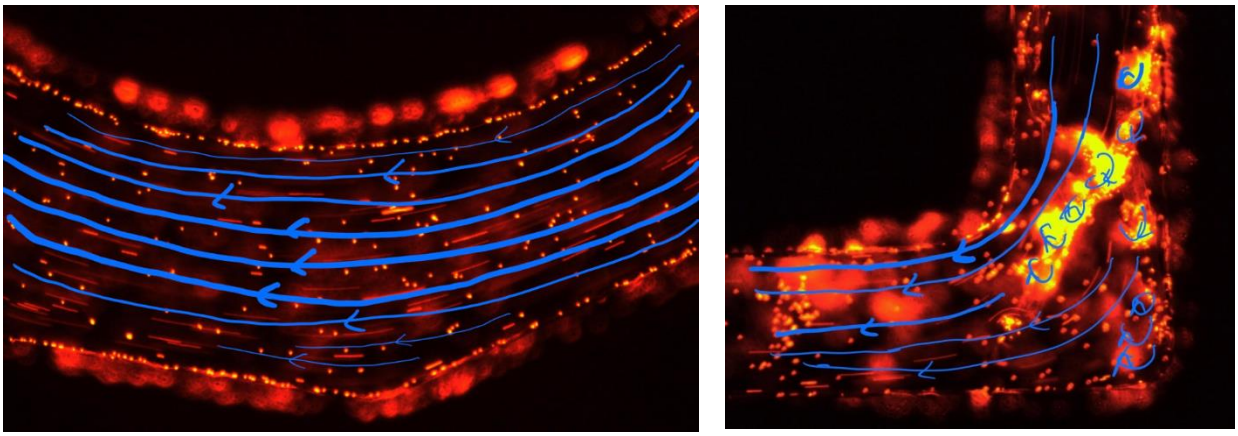

Fig. 7a (left) and 7b (right) The path of beads as they travel around the bends. The thickness of the lines roughly corresponds to the velocity of the beads. For 7a, velocity was greatest near the middle of the channel; for 7b, velocity was greatest near the top-left corner of the bend. Furthermore, the bottom right corner of 7b experienced significant turbulence, making velocity unpredictable.

Error Analysis

The major source of error was due to the inaccuracies in the pixel measurement. The uncertainty of the pixel measurement is roughly proportional to the length of the streak - it was around 2% of the streak length in pixels. For example, a streak that was measured to be 100 pixels would have a measurement error of 2 pixels. Absolute error was not used because shorter streaks were

measured while zoomed in more, and therefore had greater accuracy. Another source of error was in the accuracy of the scale, which was used, instead of the hemocytometer, to determine the lengths of streaks. The given scale was precise to the nearest whole number, so the uncertainty was $\pm 1\ \mu m$. It was assumed that the scale was accurate, namely that $100 \mu m$ as indicated on the scale was exact. However, it is impossible to verify this assumption without a hemocytometer. Finally, the exposure time was accurate to one decimal place, so its uncertainty was $\pm 0.1\ ms$. With these uncertainties, the error of the velocity calculations could be determined.

The error propagation formula is given by [3]:

If

$$Q = \frac{ab\cdots c}{xy\cdots z},$$

then

$$\frac{\delta Q}{|Q|} = \sqrt{\left(\frac{\delta a}{a}\right)^2 + \left(\frac{\delta b}{b}\right)^2 + \cdots + \left(\frac{\delta c}{c}\right)^2 + \left(\frac{\delta x}{x}\right)^2 + \left(\frac{\delta y}{y}\right)^2 + \cdots + \left(\frac{\delta z}{z}\right)^2}.$$

The formula for velocity is: $v = \frac{(s \pm 0.02s\ pixels) * (100 \pm 1 \mu m)/(613 \pm 2 pixels)}{50.6 \pm 0.1 ms}$. Using the above equation, $\delta v = \pm |v| \sqrt{(0.02s/s)^2 + (1/100)^2 + (2/613)^2 + (0.1/50.6)^2}$, where s is the measured streak length in pixels and v is the calculated velocity. This equation simplifies to $\delta v = \pm v \sqrt{0.02^2 + 0.00011455}$. The formula for the length of a streak is: $l = (s \pm 2 pixels) * (100 \pm 1 \mu m)/(613 \pm 2 pixels)$. By the same error propagation formula, $\delta l = \pm |l| \sqrt{(0.02)^2 + (1/100)^2 + (2/613)^2}$. This simplifies to $\delta l = \pm l \sqrt{0.02^2 + 0.0001106}$. From these formulas we conclude that the errors of velocity and length were directly proportional to their measurements. These errors were included as error bars in the velocity profile of channel 1 (Fig. 4).

Conclusions

This lab mainly investigated how velocity changed given different channel geometries, such as a widening channel and an abrupt bend. Furthermore, turbulent and laminar flow in different geometries and flow conditions were identified. Fluid flow is fascinating both on the macroscopic and microscopic level. In fact, observing microscopic fluid flow can give us incredible insight into fluid flow in the macroscopic world.

References

[1] Microfluidics Lab Manual v2, available: https://q.utoronto.ca/courses/239495/files/15775907?module_item_id=2923675

[2] Online Pixel Ruler, available: https://www.rapidtables.com/web/tools/pixel-ruler.html

[3] A Summary of Error Propagation, available: https://www.rapidtables.com/web/tools/pixel-ruler.html